Supplemental Information for Sun et al., "Thermally enhanced photo-induced electron emission from nitrogen-doped diamond films on silicon substrates"

Experimental Details

Prior to growth of the diamond film, the boron-doped Si substrate surface was sonicated in a nano-diamond slurry for 60 min. The sonication process was followed by an acetone rinse and nitrogen gas drying. The nucleation step was then followed by the deposition of a nitrogen-incorporated ultra-nanocrystalline diamond ((N)UNCD) layer and then a polycrystalline nitrogen-doped diamond (N-diamond) layer. The UNCD layer was deposited using 10 sccm argon, 100 sccm nitrogen and 20 sccm methane for 35 min. The N-diamond layer deposition employed hydrogen at 400 sccm, methane at 2 sccm, and nitrogen at 100 sccm for ~70 min. The diamond films had a total thickness of ~400-500 nm as determined by *in-situ* laser reflectance interferometry. After deposition, the samples were cooled in a hydrogen plasma (400 sccm hydrogen) for 1 min to obtain H-terminated surfaces. The UNCD layer has a smaller grain size and hence a higher percentage of sp^2 bonds at the grain boundary, which leads to sufficient conductivity for the diamond film. On the other hand the polycrystalline N-diamond layer provides the low effective work function through the negative electron affinity and *n*-type doping.

Electron microscopy images of the diamond samples were acquired with a JEOL ARM200F aberration corrected scanning transmission electron microscope (STEM) to examine the diamond/Si interface. The specimen preparation employed a focused ion beam (FIB) lift-out technique using a FEI Nova 200 NanoLab instrument with an Omniprobe tip. Electron microscopy of the sample (Fig. S1) indicates a smooth interface between Si and the (N)UNCD layer. A grain size of less than 10 nm is shown in the (N)UNCD layer. There is a thin layer between the two materials which has a thickness of ~ 2nm. Energy-dispersive X-ray spectroscopy (EDX) measurements indicate that this layer is likely a disordered combination of Si, C and a trace amount of oxygen.

In the electron spectroscopy system, a toroidal tungsten coil beneath the sample provided radiative heating for a temperature range of 20 to 400 ℃. The sample temperature was monitored with a thermocouple located at the center of the coil, and the

sample surface temperature was calibrated with a Mikron M90Q infrared pyrometer throughout the experiments. The vacuum pressure was maintained between 10^{-9} to 10^{-8} Torr. The band pass filters on the filtered Xe lamp have a FWHM of ~10 nm. The photon flux was estimated by measuring the radiative power density of the filtered light using a Newport 1916-C optical power meter. During measurements at the same temperature set point, the monitored temperature showed a variance of less than ±2 ℃, and the light illumination had no observable effect on the measured sample temperature. A Keithley 237 source measuring unit was employed to record the photocurrent from the diamond sample when photon illumination was provided. The measured photocurrent was typically in the range of 0.5 to 5 nA depending on the photon energy, which corresponded to an effective quantum efficiency of ~10^{-5} to 10^{-4}. Work function of the hemispherical analyzer is ~ 4.3 eV as calibrated by a standard Au foil. As this value is higher than the kinetic energy of the emitted electrons, a -10V bias was applied to the sample surface to overcome the analyzer work function. The spectra were shifted by the applied bias. Consequently, the electron energy above E_F, *KE(sample)*, is given by the following equation:

$$KE(sample) = KE(analyzer) - e \cdot V + \Phi_A, \quad (1)$$

where *KE(analyzer)* refers to the electron kinetic energy as measured by the analyzer, V the applied voltage (10V), and Φ_A the analyzer work function (4.3 eV).

Fig. S2 shows UV photoemission spectra as a function of temperature, collected from a nitrogen-doped diamond film on the p-type Si substrate. The measurements employed a He discharge lamp optimized for generation of He I (21.2 eV) photons, which were delivered to the sample surface through a ~1.5 mm diameter quartz capillary. As the photon energy is greater than the bandgap of diamond, the photoelectrons are excited from valence band states close to the diamond surface. The electrons in the conduction band lead to the photoemission spectra. Thus, the low energy cut-off of the spectra represents the effective work function Φ_W of the N-diamond surface layer. A low value (~1.9 eV) was observed, which remains approximately constant within the studied temperature regime.

Modeling Approaches

1) Photon-enhanced thermionic emission (PETE)

The following analysis is based on the work by Schwede et al. [1]. For a semiconductor which exhibits PETE, the photons with energy above the band gap will generate electrons in the conduction band and form an enhanced carrier population. This leads to a shift of the quasi-Fermi level in the semiconductor towards the CBM and consequently reduces the effective energy barrier for thermionic emission. As a result, the electron emission intensity may be significantly enhanced with photon illumination. The PETE coefficient K_{PETE} is given as:

$$K_{PETE} = \sqrt{\frac{k_B T}{2\pi m_n^*}} \exp[-\chi / k_B T], \quad (2)$$

where k_B stands for the Boltzmann constant, m_n^* the electron effective mass, and T the emitter temperature. Only the cross-gap recombination through black-body type radiation is considered here by simplification, which has a coefficient K_{BB} of:

$$K_{BB} = \frac{2\pi}{h^3 c^2 n_{eq} p_{eq}} \int_{E_G}^{\infty} \frac{(h\nu)^2 d(h\nu)}{\exp(h\nu / k_B T) - 1}, \quad (3)$$

where h stands for the Planck constant, ν the photon frequency, c the speed of light, and n_{eq} and p_{eq} the equilibrium electron and hole concentrations. Auger recombination, while neglected here, can become more significant as the electron population increases, and will need to be included for a more complete analysis.

Within the constraints of this model, the equilibrium between generation and recombination leads to the following relationship:

$$0 = (\Gamma_P - K_{PETE} n_{eq}) - (K_{PETE} + K_{BB}(n_{eq} + p_{eq}))dn - K_{BB} dn^2 . \quad (4)$$

Here Γ_P represents the photon flux, dn the enhanced electron population in the conduction band, and χ the emission barrier height with respect to the CBM. To express the analysis in a more familiar form, the photon-enhanced emission current density is given in a form similar to the Richardson-Dushman relationship for "pure" thermionic electron emission:

$$J = A^* T^2 \exp[-(\Phi - (E_{F,n} - E_F)) / k_B T] = e(n_{eq} + dn) \sqrt{\frac{k_B T}{2\pi m_n^*}} \exp[-\chi / k_B T], \quad (5)$$

2) Direct photoemission

Direct photo-electron generation in a semiconductor focuses on a non-equilibrium process, where the photo-electrons transport across the interface barrier before thermal relaxation. This emission mechanism can be simulated by employing an internal photo-emission model [2, 3], which describes the quantum yield as a function of the energy of the illuminating photons:

$$Y(h\nu)=\frac{\int_0^{h\nu-E_G}T(E)S(E,h\nu)N_c(E)N_v(E-h\nu)dE}{\int_0^{h\nu-E_G}N_c(E)N_v(E-h\nu)dE}, \quad (6)$$

where N_c and N_v are the conduction band and valence band density of states (DoS) in the absorbing substrate, respectively. The energy zero is referred to the CBM. The emitted electron function, *T(E)*, with kinetic energy *E* that exceeds the energy barrier χ is given by Fowler's assumption [3, 4] as:

$$T(E)=\frac{1}{2}\left[1-\sqrt{\frac{\chi}{E}}\right], E\geq\chi; T(E)=0, E<\chi. \quad (7)$$

The absorption function *S(E, hν)* is given in the form of:

$$S(E,h\nu)=\frac{\alpha(h\nu)L(E)}{1+\alpha(h\nu)L(E)}, \quad (8)$$

which involves *α(hν)*, the frequency dependent optical absorption coefficient of the substrate, and *L(E)*, the electron inelastic mean free path (IMFP). As Si has an indirect band gap of 1.12 eV, its optical properties in the UV and visible wavelength regimes show a significant temperature dependence. For instance, the absorption coefficient (α) of Si as a function of temperature for 400 nm light has been measured experimentally, and an empirical equation in Ref. [5] is employed in this work:

$$\alpha(h\nu)=\frac{4\pi\nu}{c}\left(-0.0805+\exp\left(-3.1893+\frac{7.946}{3.648^2-h^2\nu^2}\right)\right)\cdot\exp\left(\frac{T}{369.9-\exp\left(-12.92+5.509\cdot h\nu\right)}\right), \quad (9)$$

where c is the speed of light, T is in the unit of ℃ and hv in eV. The IMFP of low kinetic energy electrons is usually difficult to determine, and thus in this model it is assumed to be a constant ~100 nm in Si. Assuming parabolic DoS for Si and diamond, and substituting Eq. (6) and (7) into Eq. (5), the direct photo-generation spectrum using the specific diamond properties is obtained through a numerical calculation.

References

[1] J.W. Schwede, I. Bargatin, D.C. Riley, B.E. Hardin, S.J. Rosenthal, Y. Sun, F. Schmitt, P. Pianetta, R.T. Howe, Z.X. Shen, N.A. Melosh, "Photon-Enhanced Thermionic Emission for Solar Concentrator Systems", *Nat. Mater.* 9 (2010): 762-767.

[2] N.B. Kindig, W.E. Spicer, "Band Structure of Cadmium Sulfide - Photoemission Studies", *Phys. Rev.* 138 (1965): A561-576.

[3] R.J. Powell, "Interface Barrier Energy Determination from Voltage Dependence of Photoinjected Currents", *J. Appl. Phys.* 41 (1970): 2424-2432.

[4] R.H. Fowler, "The Analysis of Photoelectric Sensitivity Curves for Clean Metals at Various Temperatures", *Phys. Rev.* 38 (1931): 45.

[5] G.E. Jellison, F.A. Modine, "Optical Functions of Silicon at Elevated Temperatures", *J. Appl. Phys.* 76 (1994): 3758.

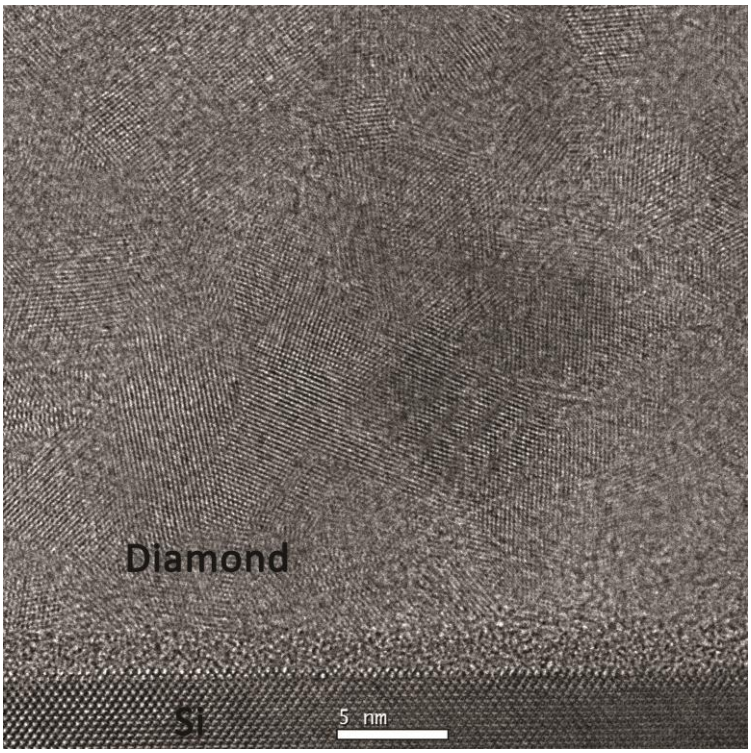

Fig. S1 High resolution electron microscopy image of the diamond/Si interface, showing the (N)UNCD layer on the top and single crystal Si substrate on the bottom.

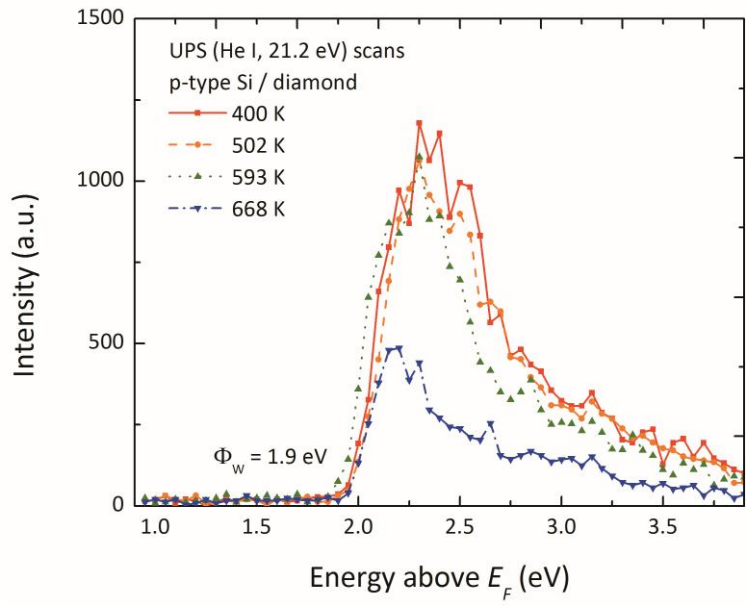

Fig. S2 UV (21.2 eV) photoemission spectra of a nitrogen-doped diamond film on a *p*-type Si substrate. Data were acquired with a ~0.02 eV resolution. An effective work function of ~1.9 eV was observed which was relatively independent of temperature.